RSC Advances

PAPER

Cite this: *RSC Adv.*, 2015, **5**, 26189

Electrospun polymer nanofiber membrane electrodes and an electrolyte for highly flexible and foldable all-solid-state supercapacitors†

Yue-E Miao, Jiajie Yan, Yunpeng Huang, Wei Fan and Tianxi Liu*

A sandwiched symmetric all-solid-state supercapacitor consisting of flexible electrospun polyaniline (PANI)/carbonized polyimide (CPI) nanocomposite membrane electrodes and a poly(vinyl alcohol) (PVA)/poly(acrylic acid) (PAA) nanofiber membrane-reinforced PVA/H_3PO_4 gel separator has been successfully fabricated. Needle-like PANI nanoparticles are vertically formed on the high electrically conductive three-dimensional CPI nanofiber network, resulting in an efficiently improved specific surface area of the PANI nanoparticles and faster electrolyte ion penetration and electron transfer in the active electrode material. The synergistic effect thus generates remarkably higher specific capacitance of 379 F g^{-1} at 0.5 A g^{-1} and longer cycle life with a retention of 94% at 1 A g^{-1} for PANI/CPI nanocomposite membrane electrodes, compared with those (209 F g^{-1}, 56%) of neat PANI powder. Furthermore, electrospun PVA/PAA nanofiber membrane-reinforced PVA/H_3PO_4 gel separator exhibits superior mechanical properties over the traditional PVA/H_3PO_4 gel separator, thus endowing the entire device with high flexibility and foldability. Therefore, electrospinning is a very promising technique for the preparation of highly flexible and foldable electrode and separator materials with hierarchical structures in high-performance new energy storage applications.

Received 5th January 2015
Accepted 6th March 2015

DOI: 10.1039/c5ra00138b

www.rsc.org/advances

1 Introduction

Recent development in portable electronics has promoted increasing demand for high-performance energy-storage systems which are ultrathin, lightweight, flexible, and even foldable or wearable.[1] Among the various energy-storage systems, supercapacitors have received much attention as an attractive class of energy-storage devices due to their high power density, fast charging and discharging rates, long cycle life, and high reliability. However, the employment of inactive components, including conductive additives, binders, and current collectors make the conventional supercapacitors still too thick, heavy, and rigid to meet the practical requirements for portable devices.[2,3] Moreover, the conventional energy-storage devices usually consist of a separator sandwiched between two electrodes sealed in a liquid electrolyte, which suffers drawbacks of electrolyte leakage and severely limits their applications in future advanced thin and wearable electronic areas. Therefore, developing high-performance all-solid-state supercapacitors which are lightweight, have high flexibility and even portability still remains an urgent task.[4,5]

Essentially, high-performance flexible supercapacitors strongly depend on the innovation of electrode materials which possess good electrical and mechanical properties, high power/energy densities, and excellent cyclic stability.[6–9] As a promising conductive polymer electrode material for supercapacitors, polyaniline (PANI) has been widely investigated due to its ease of synthesis, good environmental stability, high conductivity and theoretical specific capacitance.[10–12] However, several severe issues, such as large volume change and poor cyclability, need to be resolved in rendering PANI as electrode material for practical supercapacitor applications.[13] To address this issue, incorporating pseudocapacitance materials with carbon-based materials is a promising approach to achieve the synergistic electrochemical performances of electrochemical double-layer capacitors and pseudocapacitors.[14] Therefore, various nanostructured carbon materials with large surface area and good conductivity, such as carbon nanofibers, carbon nanotubes, and graphene, are extensively used as supporting materials to generate hierarchically architectural carbon/PANI nanocomposites with both high performance and long cycle life.[15–17] Uppugalla *et al.* have designed a hybrid composite electrode of N, S and O doped carbon with polyaniline (CNSO-PANI),[12] which yields a high capacitance of 372 F g^{-1} compared to pristine PANI (200 F g^{-1}) at 0.8 A g^{-1}. Nevertheless, mechanical deformation triggered

State Key Laboratory of Molecular Engineering of Polymers, Department of Macromolecular Science, Fudan University, Shanghai 200433, PR China. E-mail: txliu@fudan.edu.cn; Fax: +86-21-65640293; Tel: +86-21-55664197

† Electronic supplementary information (ESI) available. See DOI: 10.1039/c5ra00138b

internal short-circuit failures between electrodes is still formidable challenge for developing flexible supercapacitors, which imposes stringent limitations on achieving a satisfactory level of architectural flexibility.[18] Therefore, solid electrolytes, such as gel polymer electrolytes and proton conducting membranes, have been thoroughly explored due to several advantages over liquid ones, including easy handling without spillage of hazardous liquid, low internal corrosion, simple construction process, and flexibility in packaging.[19] Aqueous ion gel electrolytes, such as poly(vinyl alcohol) (PVA)/H_2SO_4 and PVA/H_3PO_4, have been widely used as both separator and electrolyte to construct all-solid-state supercapacitors.[20,21] In addition, both PVA and poly(acrylic acid) (PAA) have been reported as part of either polymer electrolyte or separator in flexible batteries, where PVA–KOH–water system has been reported to remain stable for a period of two years and the addition of PAA further increases ionic conductivity.[22,23] However, the formation of solid-state polymer electrolyte membrane on a Petri dish shows that its thickness could not be smaller than 0.15 mm, which severely limits the ion transmission process and dimensional miniaturization of the entire device.[24] Thus, developing new kinds of solid-state polymer electrolyte with small thickness, high flexibility and foldability is of great necessity for fabricating high-performance energy storage systems.

Electrospinning is a promising and straightforward technique that produces free-standing nanofiber membranes which are preferred as both electrodes and separators for flexible energy storage devices.[25–27] As one kind of popular electrode materials, electrospun carbon nanofibers (CNF) have been playing a leading role in supercapacitors due to their high surface area, controllable electronic conductivity and simplicity of preparation. Whereas, low power and energy density severely limits their applications, thus leading to an increasing research attention on nanocomposites of CNF and pseudocapacitance materials, such as metal oxides and conductive polymers,[28] for high-performance energy storage applications. In addition, electrospun polyacrylonitrile, poly(vinylidene fluoride) and polyimide (PI) nanofiber-based nonwovens have been developed and evaluated in lithium ion batteries, which exhibit outstanding battery performances, such as large capacity, high-rate capability and long cycle life.[29–31] Therefore, in this study highly flexible and foldable all-solid-state supercapacitor has been constructed by electrospinning *via* a simple two-step approach, that is, the formation of flexible electrospun PANI/carbonized polyimide (CPI) nanocomposite membrane electrodes and PVA/PAA nanofiber membrane-reinforced gel separator. PANI/CPI composite membrane electrodes with hierarchical structures exhibit much higher specific capacitance of 379 F g^{-1} at 0.5 A g^{-1} and longer cycle life with a retention of 94% at 1 A g^{-1} than those (209 F g^{-1}, 56%) of PANI powder under the same current densities. In addition, electrospun PVA/PAA nanofiber membrane-reinforced gel separator is not only served as an effective separator but also as a means of electrolyte storage and transportation, to ensure high flexibility and foldability for high-performance energy storage devices.

2 Experimental section

2.1 Materials

Pyromellitic dianhydride (PMDA), 4,4′-oxydianiline (ODA), and *N*,*N*-dimethylacetamide (DMAc) were commercially obtained from China Medicine Co. PVA (M_w from 85 000 to 124 000, 98–99% hydrolyzed) was purchased from Sigma-Aldrich. PAA ($M_w \sim 1800$, 25 wt% aqueous solution) was obtained from Aladdin Chemical Reagent. Aniline and ammonium persulfate (APS) were purchased from Sinopharm Chemical Reagent Co. Ltd. All other reactants were of analytical purity and used as received.

2.2 Preparation of electrospun CPI nanofiber membranes

The precursor of PI, poly(amide acid), was synthesized *via* polycondensation of PMDA and ODA with an equivalent molar ratio in DMAc at −3 °C, thus obtaining pristine poly(amide acid) solution with a solid content of 15%. Electrospinning was carried out using a syringe with a spinneret having a diameter of 0.5 mm at an applied voltage of 18–25 kV. Poly(amide acid) solution with a dilute concentration of 12 wt% was fed at a speed of 0.25 mL h^{-1} with a distance of 20 cm between tip of the needle and collector. The collected poly(amide acid) nanofiber membrane was overnight dried at 60 °C to remove the residual solvent and then thermally imidized to obtain PI nanofibers using the following program: heating up at a rate of 3 °C min^{-1} to 100, 200 and 300 °C, followed by an annealing at each temperature stage for 30 min. Then, conductive CPI nanofibers were obtained *via* a carbonization process by heating up at a rate of 5 °C min^{-1} to 1000 °C and maintaining there for 60 min.

2.3 Preparation of PANI/CPI nanocomposite membranes

In situ polymerization of aniline was carried out in an ice/water bath at the temperature of 0–5 °C according to our previous study.[32] The as-prepared CPI fiber membrane was first treated in a bath of H_2SO_4 (98 wt%) for 10 min, and thoroughly rinsed with deionized water. Then, the treated CPI nanofiber membrane was immersed in 20 mL 1 M HCl solution containing aniline for sufficient adsorption of aniline. Another 20 mL 1 M HCl solution containing APS was slowly added into the above solution to initiate the polymerization. Different aniline concentrations of 0.0025 M, 0.005 M, 0.015 M, and 0.03 M were used for polymerization over 12 h respectively, with the molar ratio of aniline/APS fixed at 2/1. Thus, CPI/PANI composite nanofiber membranes were obtained with increasing aniline concentrations and correspondingly labelled as 0.0025 M, 0.005 M, 0.015 M and 0.03 M CPI/PANI as shown in Fig. 1. Meanwhile, PANI powder without the CPI membrane template was *in situ* polymerized under the same condition for a comparative study.

2.4 Preparation of electrospun PVA/PAA nanofiber membrane-reinforced gel separator

10 wt% of PVA and 12 wt% of PAA aqueous solutions were mixed with a volume ratio of 1 : 1, and further stirred at room temperature for 1 h to obtain a homogeneous solution for

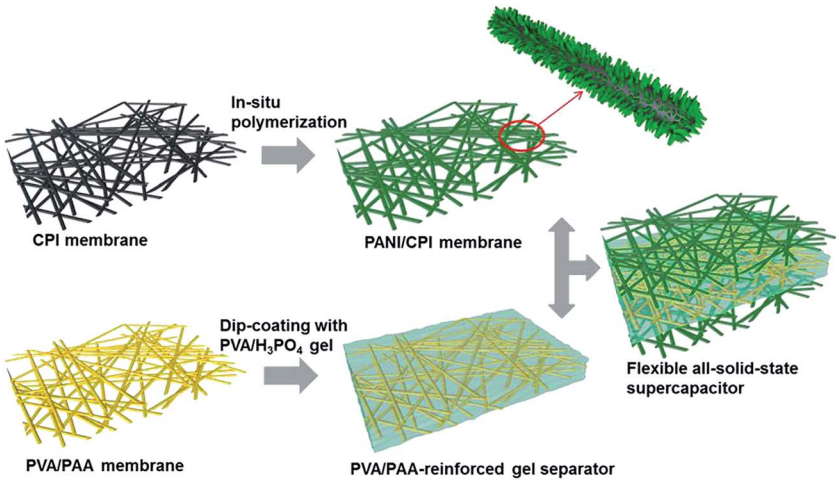

Fig. 1 Schematic for the preparation of flexible and foldable all-solid-state supercapacitors consisting of electrospun PANI/CPI composite membranes and PVA/PAA nanofiber membrane-reinforced gel separator.

electrospinning at a voltage of 15 kV and a feeding rate of 0.5 mL h^{-1}. The electrospun PVA/PAA nanofiber membranes thus obtained were carefully detached from the aluminum collector and dried in vacuum at room temperature for 24 h. After that, the temperature was raised and maintained at 120 °C for 3 h for heat-induced crosslinking reaction between PVA and PAA. Thus, crosslinked electrospun PVA/PAA membrane was obtained for dip-coating with PVA/H_3PO_4 gel solution (with a solid content of 10 wt%) to obtain PVA/PAA nanofiber membrane-reinforced gel separator (Fig. 1).

2.5 Characterization

Morphologies of PI and CPI fiber membranes, PANI/CPI and PVA/PAA composite fiber membranes were investigated by field-emission scanning electron microscope (FESEM, Ultra 55, Zeiss). All electrochemical experiments were carried out on a CHI 660D electrochemical workstation at room temperature. In the two-electrode system, CPI or PANI/CPI fiber membranes were used as two working electrodes as well as current collectors while electrospun PVA/PAA nanofiber membrane-reinforced PVA/H_3PO_4 gel membrane was directly used as separator, thus forming highly flexible and foldable all-solid-state supercapacitors. Cyclic voltammetry (CV) curves were obtained in the potential range of −0.2 to 0.8 V by varying the scan rate from

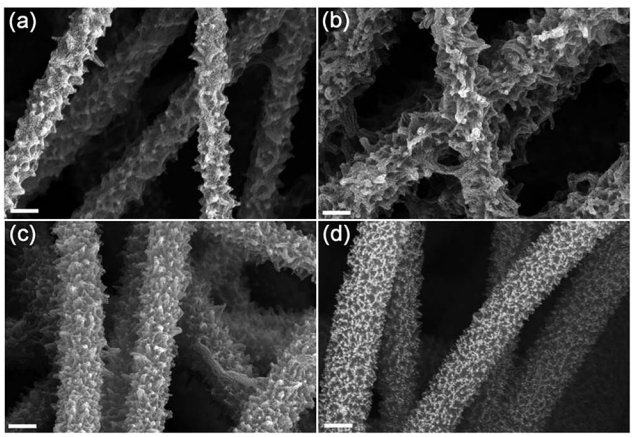

Fig. 3 High magnification FESEM images of 0.0025 M PANI/CPI (a), 0.005 M PANI/CPI (b), 0.015 M PANI/CPI (c), and 0.03 M PANI/CPI (d) composite fibers. Scale bar: 200 nm.

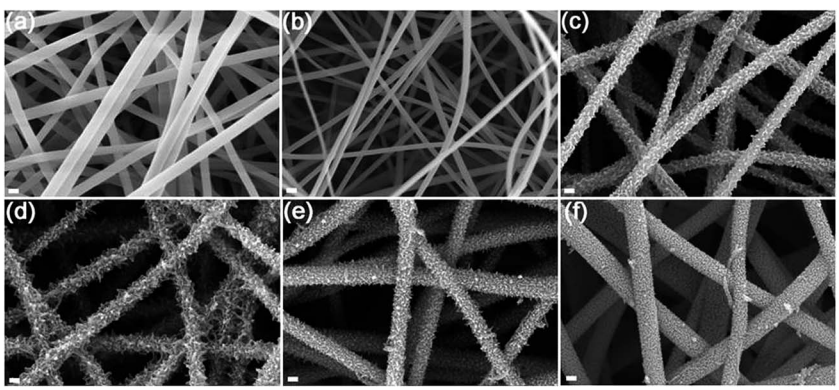

Fig. 2 FESEM images of electrospun PI (a) and CPI (b) fibers, 0.0025 M PANI/CPI (c), 0.005 M PANI/CPI (d), 0.015 M PANI/CPI (e), and 0.03 M PANI/CPI (f) composite fibers. Scale bar: 200 nm.

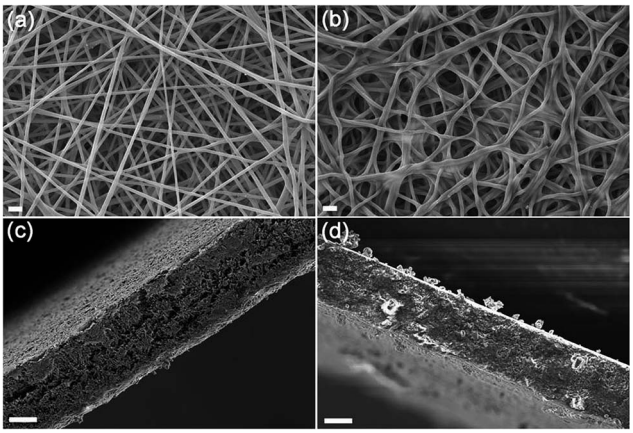

Fig. 4 FESEM images and the corresponding cross sections for electrospun PVA/PAA nanofiber membrane (a and c) and PVA/PAA nanofiber membrane-reinforced gel separator (b and d), respectively. Scale bar: 1 and 10 μm for (a and b) and (c and d), respectively.

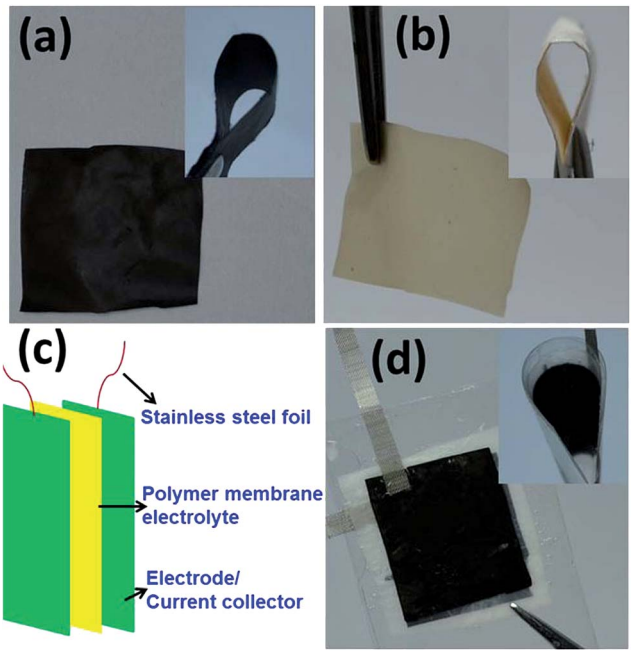

Fig. 5 Digital photographs of 0.005 M PANI/CPI composite membrane (a) and PVA/PAA nanofiber membrane-reinforced gel separator (b); schematic and digital photographs of the entire device (c and d).

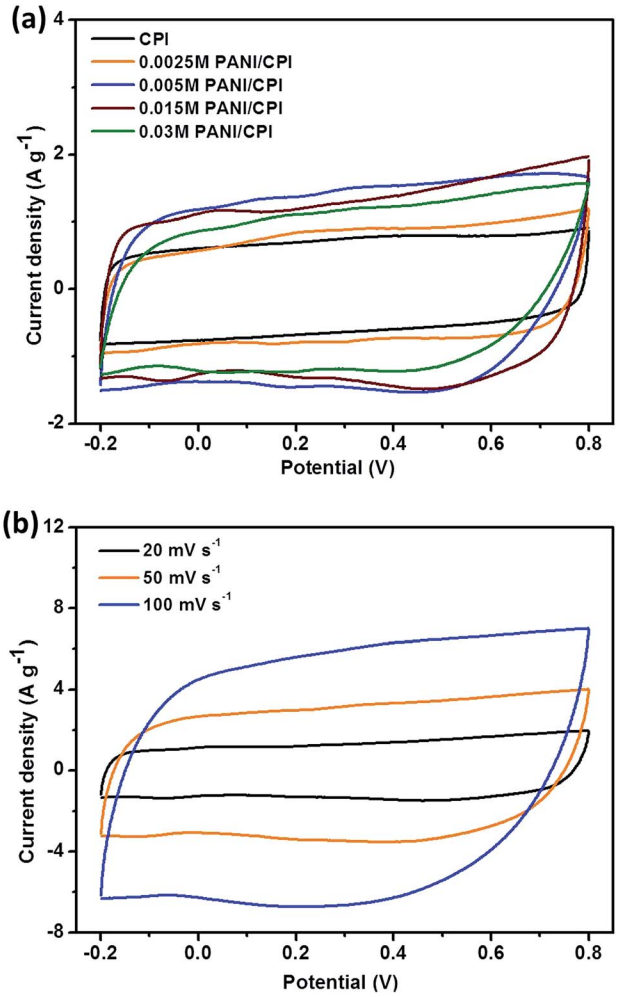

Fig. 6 (a) CV curves of supercapacitors based on CPI and PANI/CPI fiber membranes at scan rate of 20 mV s^{-1} from −0.2 to 0.8 V; (b) CV curves of supercapacitor based on 0.005 M PANI/CPI composite fiber membrane at different scan rates from −0.2 to 0.8 V.

20 to 100 mV s^{-1}. Galvanostatic charge–discharge measurements were carried out by chronopotentiometry (CP) at 0.5 to 2.5 A g^{-1}. The capacitance of CPI or PANI/CPI electrode materials was calculated from the discharge curves based on the two-electrode system, according to the equation $C_s = 4I \times \Delta t/(m \times \Delta V)$,[33] where C_s is the specific capacitance, I is the constant discharge current, Δt is the discharge time, m is the total mass of CPI or PANI/CPI composite membranes in two electrodes, and ΔV is the discharge voltage. For PANI powder, all electrochemical tests were carried out in a three-electrode system, where PANI powder was directly coated on glassy carbon electrode and used as the working electrode, platinum foil as the counter electrode, Ag/AgCl electrode as reference electrode, and 1.0 M H_2SO_4 aqueous solution as electrolyte. The capacitance was calculated according to the three-electrode system equation $C_s = I \times \Delta t/(m \times \Delta V)$,[34] where m is the mass of PANI powder in a single electrode. Electrochemical impedance measurements were performed at amplitude of 5 mV over a frequency range of 10^{-2} to 10^5 Hz. Flexibility and foldability of the all-solid-state supercapacitor were demonstrated by CV and charge–discharge tests at different bending angles.

3 Results and discussion

3.1 Physical properties of the electrospun polymer nanofiber membrane electrodes and electrolyte

Morphology and fiber diameters of PI and CPI fibers were shown in Fig. 2a and b. Diameters of the as-prepared PI and CPI nanofibers are uniform with an average size of about 200 and

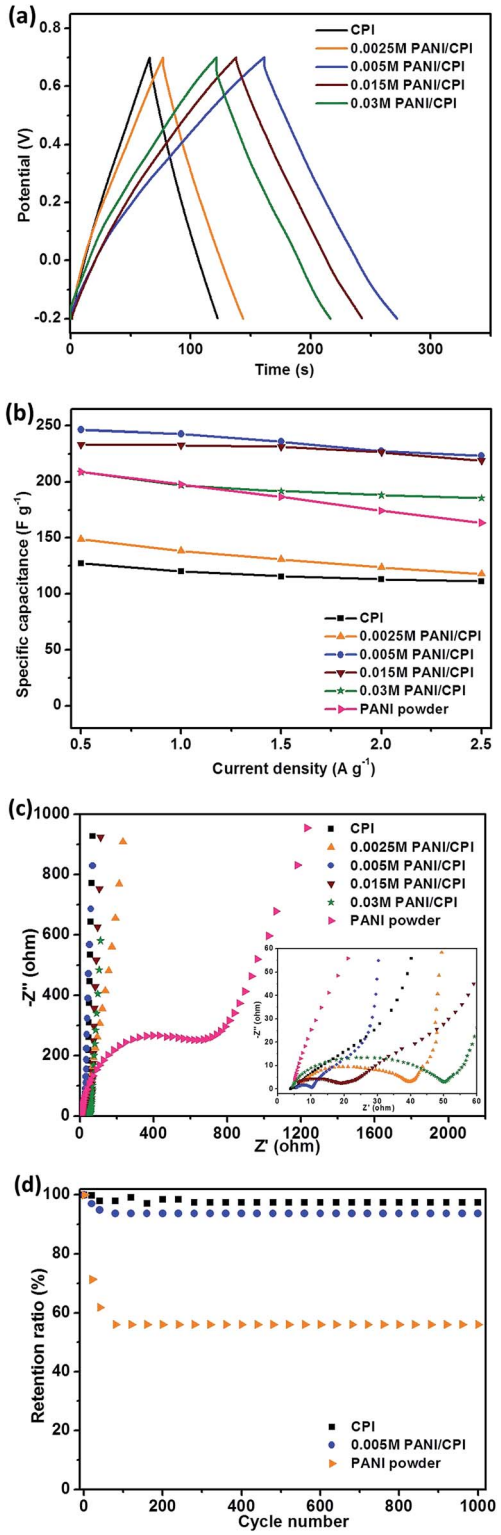

Fig. 7 (a) Charge–discharge curves at a current density of 0.5 A g^{-1}, and (b) specific capacitance plots at different current densities of supercapacitors based on CPI and PANI/CPI fiber membranes in a two-electrode system and PANI powder in a three-electrode system, respectively; (c) Nyquist impedance plots in the frequency range of 10^{-2} to 10^{5} Hz. The inset shows magnified view of high frequency region of the impedance spectra. (d) Plots of cycle life tests of supercapacitors based on PANI powder, CPI and 0.005 M PANI/CPI fiber membrane at a current density of 1 A g^{-1}.

150 nm, respectively. It can be seen that the surface of electrospun PI nanofibers is smooth and almost free of defects such as beads, which is of vital importance to provide nonwovens with good mechanical strength. Moreover, no obvious change can be observed on CPI fibers even after a high-temperature carbonization process, making them good template for further growth of PANI. FESEM images of PANI/CPI composite nanofiber membranes with different loading amount of PANI were shown in Fig. 2c–f. After *in situ* polymerization of aniline, a thin layer of PANI is grown onto the surface of CPI fibers to form a coaxial structure, with diameters of about 250 nm, 300 nm, 320 nm and 400 nm for 0.0025 M, 0.005 M, 0.015 M and 0.03 M PANI/CPI composite nanofibers, respectively. Thus, the thicknesses of PANI layers on CPI fibers are calculated to be 50 nm, 75 nm, 85 nm and 125 nm, respectively. Therefore, the wall thickness of PANI layers can be well controlled by adjusting the initial concentration of aniline. It can be seen that, however, large PANI agglomerates are gradually formed when the initial concentration of aniline increases over 0.015 M, which may be attributed to the rapid nucleation and polymerization of aniline in solution. FESEM images at high magnification clearly show the morphology and distribution of PANI on the surface of CPI fibers (Fig. 3). Needle-like PANI nanoparticles are uniformly formed even with joints between each other under certain concentrations (0.005 M and 0.015 M) of aniline (Fig. 3b and c), which could provide extremely large specific surface area of electrodes and facilitate full use of the large pseudocapacitance of PANI. XRD was employed to monitor the structures of PANI powder, CPI and PANI/CPI fiber membranes. As shown in Fig. S1,† the diffraction peaks at $2\theta = 9.8°$ and 15.3° assigned to the characteristic repeating units and doping diffraction peaks of PANI, as well as the peaks centered at $2\theta = 20.9°$ and 25.9° ascribed to the periodicity parallel and perpendicular to PANI chains, demonstrate the successful *in situ* polymerization of aniline on CPI nanofiber template. FTIR spectra further confirm the formation of PANI as shown in Fig. S2.† The characteristic peaks at 1568 cm^{-1} and 1482 cm^{-1} are attributed to the C–C stretching of the quinonoid (Q) and benzenoid (N) rings of PANI, respectively. Moreover, the bands at 1292 cm^{-1} and 1243 cm^{-1} are assigned to the C–N stretching of the benzenoid ring of PANI.

Since strong interfacial interactions can usually be achieved by using homogeneity self-reinforcement strategy for making high performance polymer composites according to our previous study,[35] electrospun PVA/PAA nanofiber membrane-reinforced PVA/H_3PO_4 gel separator is obtained here. Fig. 4 shows morphology of the surfaces and the corresponding cross sections for electrospun PVA/PAA nanofiber membrane and dried PVA/PAA nanofiber membrane-reinforced PVA/H_3PO_4 gel separator, respectively. It can be observed that the original PVA/PAA nanofibers show smooth surface and uniform morphology with a narrow fiber diameter distribution of 200–300 nm while PVA/PAA nanofiber membrane-reinforced PVA/H_3PO_4 gel separator still keeps high porosity and permeability. Moreover, the original PVA/PAA nanofiber membrane shows a thickness of 24 μm while that of PVA/PAA nanofiber membrane-reinforced PVA/H_3PO_4 gel separator decreases to

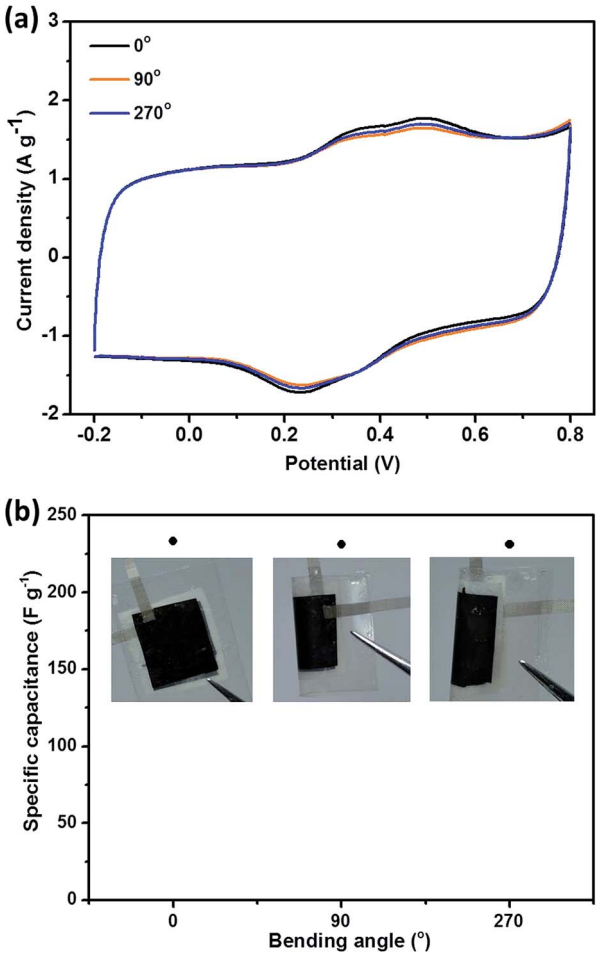

Fig. 8 (a) CV curves obtained at different bending angles of the flexible supercapacitor based on 0.005 M PANI/CPI composite membrane after 1000 cycle tests (at scan rate of 20 mV s^{-1} from −0.2 to 0.8 V); (b) the corresponding specific capacitances at different bending angles obtained at a current density of 0.5 A g^{-1}.

less than 20 μm due to good wettability and infiltration of PVA/PAA nanofiber membrane by PVA/H_3PO_4 gel solution. As thickness of the separator should be as thin as possible to decrease internal resistance and facilitate fast ion transportation at electrode/electrolyte interface, PVA/PAA nanofiber membrane-reinforced PVA/H_3PO_4 gel separator shows great potential as the middle polymer electrolyte for supercapacitors.

Furthermore, both of PANI/CPI composite nanofiber membrane (Fig. 5a) and PVA/PAA nanofiber membrane-reinforced PVA/H_3PO_4 gel separator (Fig. 5b) show great flexibility and foldability with no crack appearing upon bending. According to the schematic shown in Fig. 5c, highly flexible and foldable all-solid-state supercapacitors can be obtained by a facile construction between PANI/CPI composite nanofiber membrane and PVA/PAA nanofiber membrane-reinforced PVA/H_3PO_4 gel separator (Fig. 5d). Thus, an entire energy storage device, macroscopically, is obtained to show superior flexibility, which can be bent, twisted, and even rolled up without any cracking.

3.2 Electrochemical properties of the flexible and foldable all-solid-state supercapacitors

Electrochemical performances of all the devices were evaluated at room temperature. CV measurements were performed to study the capacitive performance of PANI powder, CPI membrane and PANI/CPI nanocomposite electrodes (Fig. 6 and S3†). Ideal electrochemical double-layer capacitance characteristic is observed from the CV curve of CPI membrane, while both PANI/CPI nanocomposite membrane and PANI powder exhibit obvious pseudocapacitance characteristics and imply the reversible charge–discharge behavior of PANI by displaying two pairs of redox peaks (P_1/P_3, P_2/P_4) (Fig. 6a and S3a†). The ideal pseudocapacitor-like behavior can be attributed to the redox transformations of PANI: the leucoemeraldine–emeraldine (P_1/P_3) and emeraldine–pernigraniline (P_2/P_4) transformations.[32] Moreover, the peak currents of all PANI/CPI nanocomposite membranes are higher than that of CPI membrane, indicating an obviously improved capacitance after the combination with pseudocapacitance materials. It can be observed that the 0.005 M and 0.015 M PANI/CPI composite membranes show higher current densities compared with those of 0.0025 M and 0.03 M PANI/CPI composite membranes. As aforementioned, needle-like PANI nanoparticles are uniformly formed even with joints between each other on the 0.005 M and 0.015 M PANI/CPI composite membranes (Fig. 3b and c), which can result in higher surface area and better utilization of pseudocapacitive PANI. CV curves of 0.005 M PANI/CPI composite membrane at different scan rates from 20 to 100 mV s^{-1} (Fig. 6b) were performed in the given potential range. With the increase of scan rate, cathodic peaks (P_1, P_2) shift positively and anodic peaks (P_3, P_4) shift negatively, respectively, indicating good rate ability and ideal capacitance behavior for PANI/CPI composite membrane electrodes.

Charge–discharge performance is investigated by CP in the potential range of −0.2 to 0.7 V. As shown in Fig. 7a and S3b,† symmetry of all the charge and discharge curves reveals good capacitance characteristics. According to the capacitance equation evaluated from the discharge curves, specific capacitances are respectively calculated to be 127, 149, 247, 233 and 209 F g^{-1} for CPI, 0.0025 M, 0.005 M, 0.015 M, and 0.03 M PANI/CPI fiber membranes at 0.5 A g^{-1} in the two-electrode all-solid-state supercapacitors, while that of PANI powder is calculated to be 209 F g^{-1} in a three-electrode system under the same current density. By the mass difference of the membrane before and after loading of PANI, the loading amount of PANI on CPI fibers has been obtained as 35.9, 47.6, 60.5 and 71.4 wt% for the 0.0025 M, 0.005 M, 0.015 M, and 0.03 M PANI/CPI fiber membranes, respectively. According to Ghosh's study,[36] the specific capacitances based on the mass of active PANI materials in PANI/CPI fiber membrane electrodes can be respectively calculated to be 188, 379, 303 and 242 F g^{-1}, which are much higher than that of neat PANI powder (209 F g^{-1}) except for 0.0025 M PANI/CPI fiber membrane. The rate capability is investigated under different charge–discharge current densities as shown in Fig. 7b. The capacitances of PANI powder, CPI and PANI/CPI fiber membranes all decrease with increasing the

current density as ions can only penetrate into the inner surface of the relatively large pores and less active surface area of the electrode material takes part in the charge–discharge process.[37] Nevertheless, almost all of PANI/CPI composite fiber membranes still keep high retention efficiency over 80% even under a high current density of 2.5 A g^{-1}. To further study the internal resistance of PANI powder, CPI and PANI/CPI fiber membrane electrodes, electrochemical impedance spectroscopy measurements were conducted as shown in Fig. 7c. It can be observed that Nyquist plots of these electrodes consist of a distorted semicircle in the high frequency region followed by a 45° sloped line and a straight line in the low frequency region, where the intercepts in the high frequency region are equal to solution resistances and diameters of the semicircles represent the electrode resistances arising from the charge transfer resistance in PANI.[38] Accordingly, the charge transfer resistances of CPI, 0.0025 M, 0.005 M, 0.015 M and 0.03 M PANI/CPI fiber membranes are 2 Ω, 32 Ω, 5 Ω, 13 Ω, and 46 Ω, respectively, which are much lower than that (600 Ω) of neat PANI powder electrode. In addition, the more vertical lines in low frequency region of CPI and 0.005 M PANI/CPI fiber membranes than that of PANI powder indicates better capacitive behavior and lower diffusion resistance of ions. The effectively decreased resistance of PANI/CPI fiber membranes can be attributed to the synergistic effect between the highly electrical conductive three-dimensional carbon nanofiber network and novel hierarchical three-dimensional micro/nano-architecture, which can efficiently improve the specific surface area of PANI nanoparticles, and facilitate electrolyte ion penetration and electron transfer in the active electrode materials. Therefore, the 0.005 M PANI/CPI fiber membrane with the lowest charge transfer resistance exhibits the highest specific capacitance.

Cycle life tests of PANI powder, CPI and 0.005 M PANI/CPI fiber membranes were conducted by galvanostatic charge–discharge measurements at a current density of 1 A g^{-1}. As shown in Fig. 7d, the 0.005 M PANI/CPI fiber membrane electrode keeps a higher retention ratio of 94% compared with that (56%) of PANI powder electrode after 1000 cycles. The electrospun CPI fiber membrane template here effectively avoids the volume expansion and collapse of PANI during the charge–discharge processes, thus resulting in a good stability and lifetime of the all-solid-state supercapacitor. Furthermore, the electrochemical capacitance of 0.005 M PANI/CPI fiber membrane electrode was measured again after cycle life tests. As shown in Fig. 8a, no significant difference can be observed from the CV curves under various deformations with obvious pseudocapacitance characteristics of PANI at a scan rate of 20 mV s^{-1}. The 0.005 M PANI/CPI fiber membrane electrode after 1000 cycles is measured to keep a specific capacitance of 231 F g^{-1} at 0.5 A g^{-1} under different bending angles as shown in Fig. 8b, further demonstrating the good stability, high flexibility and foldability of the symmetric electrochemical capacitor device. This can be attributed to the efficient homogeneity self-reinforcement by electrospun PVA/PAA nanofiber membrane during the fabrication of thin all-solid-state PVA/H_3PO_4 separator, as well as the high flexibility and foldability of electrospun PANI/CPI fiber membranes.

4 Conclusions

A sandwiched symmetric all-solid-state supercapacitor consisting of flexible electrospun PANI/CPI nanocomposite membrane electrodes and PVA/PAA nanofiber membrane-reinforced PVA/H_3PO_4 gel separator has been fabricated. Needle-like PANI nanoparticle coated high electrically conductive three-dimensional CPI nanofiber network has been constructed to achieve the synergistic effect of efficiently improved specific surface area of PANI nanoparticles and facilitated electrolyte ion penetration and electron transfer in the active electrode material. Therefore, the PANI/CPI nanocomposite membrane electrode exhibits high specific capacitance of 379 F g^{-1} at 0.5 A g^{-1} and long cycle life with a retention of 94% at 1 A g^{-1}. Moreover, electrospun PVA/PAA nanofiber membrane-reinforced PVA/H_3PO_4 gel separator exhibits good mechanical properties with high flexibility and foldability, making it promising for separator as well as electrolyte storage and transportation applications. Thus, electrospinning can be an outstanding technique to construct and prepare highly flexible and foldable electrode and separator materials with hierarchical structures for applications in high-performance new energy storage devices.

Acknowledgements

The authors are grateful for the financial support from the National Natural Science Foundation of China (51125011, 51373037, 51433001).

Notes and references

1 G. H. Yu, X. Xie, L. J. Pan, Z. Bao and Y. Cui, *Nano Energy*, 2013, **2**, 213–234.
2 Z. Q. Niu, W. Y. Zhou, J. Chen, G. X. Feng, H. Li, W. J. Ma, J. Z. Li, H. B. Dong, Y. Ren, D. Zhao and S. S. Xie, *Energy Environ. Sci.*, 2011, **4**, 1440–1446.
3 Y. M. He, W. J. Chen, C. T. Gao, J. Y. Zhou, X. D. Li and E. Q. Xie, *Nanoscale*, 2013, **5**, 8799–8820.
4 P. Simon and Y. Gogotsi, *Nat. Mater.*, 2008, **7**, 845–854.
5 H. Nishide and K. Oyaizu, *Science*, 2008, **319**, 737–738.
6 C. Choi, J. A. Lee, A. Y. Choi, Y. T. Kim, X. Lepró, M. D. Lima, R. H. Baughman and S. J. Kim, *Adv. Mater.*, 2014, **26**, 2059–2065.
7 Y. Gao, V. Presser, L. Zhang, J. J. Niu, J. K. McDonough, C. R. Pérez, H. Lin, H. Fong and Y. Gogotsi, *J. Power Sources*, 2012, **201**, 368–375.
8 Y. W. Cheng, S. T. Lu, H. B. Zhang, C. V. Varanasi and J. Liu, *Nano Lett.*, 2012, **12**, 4206–4211.
9 J. Chen, C. Jia and Z. Wan, *Electrochim. Acta*, 2014, **121**, 49–56.
10 M. K. Liu, Y. E. Miao, C. Zhang, W. W. Tjiu, Z. B. Yang, H. S. Peng and T. X. Liu, *Nanoscale*, 2013, **5**, 7312–7320.
11 C. Zhang, W. W. Tjiu and T. X. Liu, *Polym. Chem.*, 2013, **4**, 5785–5792.
12 S. Uppugalla, U. Male and P. Srinivasan, *Electrochim. Acta*, 2014, **146**, 242–248.

13 X. Zhao, B. M. Sanchez, P. J. Dobson and P. S. Grant, *Nanoscale*, 2011, **3**, 839–855.
14 E. Frackowiak, *Phys. Chem. Chem. Phys.*, 2007, **9**, 1774–1785.
15 X. B. Yan, Z. X. Tai, J. T. Chen and Q. J. Xue, *Nanoscale*, 2011, **3**, 212–216.
16 V. H. R. de Souza, M. M. Oliveira and A. J. G. Zarbin, *J. Power Sources*, 2014, **260**, 34–42.
17 W. Fan, C. Zhang, W. W. Tjiu, K. P. Pramoda, C. B. He and T. X. Liu, *ACS Appl. Mater. Interfaces*, 2013, **5**, 3382–3391.
18 K. H. Choi, S. J. Cho, S. H. Kim, Y. H. Kwon, J. Y. Kim and S. Y. Lee, *Adv. Funct. Mater.*, 2014, **24**, 44–52.
19 C. K. Subramaniam, C. S. Ramya and K. Ramya, *J. Appl. Electrochem.*, 2011, **41**, 197–206.
20 Y. N. Meng, Y. Zhao, C. G. Hu, H. H. Cheng, Y. Hu, Z. P. Zhang, G. Q. Shi and L. T. Qu, *Adv. Mater.*, 2013, **25**, 2326–2331.
21 Z. Q. Niu, L. Zhang, L. Liu, B. W. Zhu, H. B. Dong and X. D. Chen, *Adv. Mater.*, 2013, **25**, 4035–4042.
22 A. M. Gaikwad, G. L. Whiting, D. A. Steingart and A. C. Arias, *Adv. Mater.*, 2011, **23**, 3251–3255.
23 G. M. Wu, S. J. Lin and C. C. Yang, *J. Membr. Sci.*, 2006, **275**, 127–133.
24 M. Kaempgen, C. K. Chan, J. Ma, Y. Cui and G. Gruner, *Nano Lett.*, 2009, **9**, 1872–1876.
25 Z. Zhou and X. F. Wu, *J. Power Sources*, 2014, **262**, 44–49.
26 Z. P. Zhou, X. F. Wu and H. Q. Hou, *RSC Adv.*, 2014, **4**, 23622–23629.
27 N. Wu, Q. Cao, X. Y. Wang, S. Li, X. Y. Li and H. Y. Deng, *J. Power Sources*, 2011, **196**, 9751–9756.
28 S. J. He, X. W. Hu, S. L. Chen, H. Hu, M. Hanif and H. Q. Hou, *J. Mater. Chem.*, 2012, **22**, 5114–5120.
29 Y. Y. Zhai, N. Wang, X. Mao, Y. Si, J. Y. Yu, S. S. Al-Deyab, M. El-Newehy and B. Ding, *J. Mater. Chem. A*, 2014, **2**, 14511–14518.
30 T. H. Cho, M. Tanaka, H. Onishi, Y. Kondo, T. Nakamura, H. Yamazaki, S. Tanase and T. Sakai, *J. Power Sources*, 2008, **181**, 155–160.
31 Y. E. Miao, G. N. Zhu, H. Q. Hou, Y. Y. Xia and T. X. Liu, *J. Power Sources*, 2013, **226**, 82–86.
32 Y. E. Miao, W. Fan, D. Chen and T. X. Liu, *ACS Appl. Mater. Interfaces*, 2013, **5**, 4423–4428.
33 M. K. Liu, W. W. Tjiu, J. S. Pan, C. Zhang, W. Gao and T. X. Liu, *Nanoscale*, 2014, **6**, 4233–4242.
34 A. L. M. Reddy and S. Ramaprabhu, *J. Phys. Chem. C*, 2007, **111**, 7727–7734.
35 D. Chen, R. Y. Wang, W. W. Tjiu and T. X. Liu, *Compos. Sci. Technol.*, 2011, **71**, 1556–1562.
36 A. Ghosh, E. J. Ra, M. Jin, H. K. Jeong, T. H. Kim, C. Biswas and Y. H. Lee, *Adv. Funct. Mater.*, 2011, **21**, 2541–2547.
37 Z. L. Wang, R. Guo, G. R. Li, H. L. Lu, Z. Q. Liu, F. M. Xiao, M. Zhang and Y. X. Tong, *J. Mater. Chem.*, 2012, **22**, 2401–2404.
38 K. Zhang, L. L. Zhang, X. S. Zhao and J. S. Wu, *Chem. Mater.*, 2010, **22**, 1392–1401.